Vol 17 No 1, January 2008
1674-1056/2008/17(01)/0264-06

Chinese Physics B

© 2008 Chin. Phys. Soc.
and IOP Publishing Ltd

Shear modulus of shock-compressed LY12 aluminium up to melting point*

Yu Yu-Ying(俞宇颖)†, Tan Hua(谭 华),
Hu Jian-Bo(胡建波), and Dai Cheng-Da(戴诚达)

Laboratory for Shock Wave and Detonation Physics Research, Institute of Fluid Physics, China Academy of Engineering Physics, Mianyang 621900, *China*

(Received 11 January 2007; revised manuscript received 24 September 2007)

Asymmetric plate impact experiments are conducted on LY12 aluminium alloy in a pressure range of 85–131 GPa. The longitudinal sound speeds are obtained from the time-resolved particle speed profiles of the specimen measured with Velocity Interferometer System for Any Reflector (VISAR) technique, and they are shown to be good agreement with our previously reported data of this alloy in a pressure range of 20–70 GPa, and also with those of 2024 aluminium reported by McQueen. Using all of the longitudinal speeds and the corresponding bulk speeds calculated from the Gruneisen equation of state (EOS), shear moduli of LY12 aluminium alloy are obtained. A comparison of the shear moduli in the solid phase region with those estimated from the Steinberg model demonstrate that the latter are systematically lower than the measurements. By re-analysing the pressure effect on the shear modulus, a modified equation is proposed, in which the pressure term of $P/\eta^{1/3}$ in the Steinberg model is replaced by a linear term. Good agreement between experiments and the modified equation is obtained, which implies that the shear modulus of LY12 aluminium varies linearly both with pressure and with temperature throughout the whole solid phase region. On the other hand, shear modulus of aluminium in a solid-liquid mixed phrase region decreases gradually and smoothly, a feature that is very different from the drastic dropping at the melting point under static conditions.

Keywords: shear modulus, Steinberg model, shock compression, melting point, LY12 aluminium
PACC: 6250, 6220, 4630M

1. Introduction

Shear modulus is an important material parameter needed to implement the constitutive laws.[1,2] A good understanding of shear modulus over a wide range of pressure and temperature is therefore essential to shock dynamic simulations of materials subjected to strong shock loadings.

For an isotropic material, shear modulus G is generally determined from the sound speed measurements by the well-known relationship

$$G = \rho c_{\mathrm{t}}^2 = \frac{3}{4}\rho\left(c_{\mathrm{l}}^2 - c_{\mathrm{b}}^2\right), \tag{1}$$

where ρ is the instant density, c_{t}, c_{l} and c_{b} are the shear, the longitudinal and the bulk sound speed, respectively. Therefore measurements of sound speeds in solids at different pressures and temperatures will yield the full information about the variations of shear modulus.

While ultrasonic method is commonly used to determine the longitudinal and the shear speeds, this approach is usually limited to a static condition and a relatively low pressure regime.[3,4] Sound speeds of materials in high-pressure and high-temperature states are commonly measured in shock experiments by measuring the speeds of catch-up rarefaction wave behind the shock front. For solids, the propagation of the wave front of this rarefaction wave is assumed to travel at a longitudinal sound speed. Various approaches, including optical analyser method,[5,6] manganin gauge method,[7,8] velocity interferometer system for any reflector (VISAR) technique[9] and Doppler Laser Interferometry (DLI) technique,[10] have been applied to measuring the sound speeds in shock-compressed materials during the last 20 years. Of these techniques, VISAR has recently been used most frequently because this non-contact probing technique provides us a direct measurement of the

*Project supported by the National Natural Science Foundation of China (Grant Nos 10232040 and 10672149) and the foundation of Laboratory for Shock Wave and Detonation Physics Research, China Academy of Engineering Physics (Grant No 9140C6702020603).

†E-mail: yuyinyu@21cn.com

mass movement speed history over a wide pressure range and it is also very convenient to deduce the sound speed from the sample–window interface particle speed history.[11−15]

LY12 aluminium alloy (similar to 2024 aluminium of USA designation) is a standard material used for equation of state (EOS) measurements in shock wave experiments. A better knowledge about its sound speed and shear modulus over a wide shock pressure range is of considerable significance. We[16] have reported the longitudinal and the bulk sound speeds of this alloy over a pressure range of 20–70 GPa resulting from symmetric impact experiments with VISAR technique. While these data exhibit a satisfactory accuracy, they are limited to a relatively low pressure regime because of the low impedance of LY12 aluminium alloy.

In the present work, asymmetric plate impact experiments on LY12 aluminium are carried out over a pressure range from 85 to131 GPa. Time-resolved particle speed profiles obtained from VISAR measurements are used to determine the longitudinal sound speed of shocked LY12 aluminium samples. The shear moduli of LY12 aluminium in a pressure range of 20–131 GPa are determined using the sound speed data of the present work and our previous data in Ref.[16]. A comparison of the experimental results, including the data of 2024 aluminium from McQueen *et al*,[17] with those calculated from the widely used shear modulus model developed by Steinberg *et al*[1] is also made.

2. Experimental technique

The commercial LY12 aluminium materials used in the present investigation is of the same batch as those used in our previous experiments.[16] The chemical compositions in weight percentages are as follows: Al: 95.15–96.95, Cu: 3.8–4.9, Mg: 1.2–1.8, Mn: 0.3–0.9, Ti: $\leq$ 0.5, Zn: $\leq$ 0.3, Fe: $\leq$ 0.5, Si: $\leq$ 0.5, Ni: $\leq$ 0.5. The Hugoniot parameters of this alloy have been carefully measured and are the same as those of 2024 aluminium given by Marsh.[18]

Plate impact experiments were conducted by using the two-stage light-gas gun at Laboratory for Shock Wave and Detonation Physics Research. A magnetic-particle-velocimeter was used to measure the projectile velocity with an uncertainty better than 0.2%. The basic experimental configuration is shown in Fig.1(a). High impedance 304 steel or tantalum plates were chosen as the flyer to impact the LY12 aluminium sample, which has a transparent single crystal lithium fluoride (LiF) window to maintain the sample under high pressure compression. Dimensions of the flyers, samples and windows were designed to assure that the uniaxial strain condition could be maintained during the whole unloading process in sample. The particle speed profiles at the sample–window interface were measured by using VISAR technique.[9] To yield unambiguous particle speed histories from the VISAR records, three different fringe constants were used in each experiment in this study.

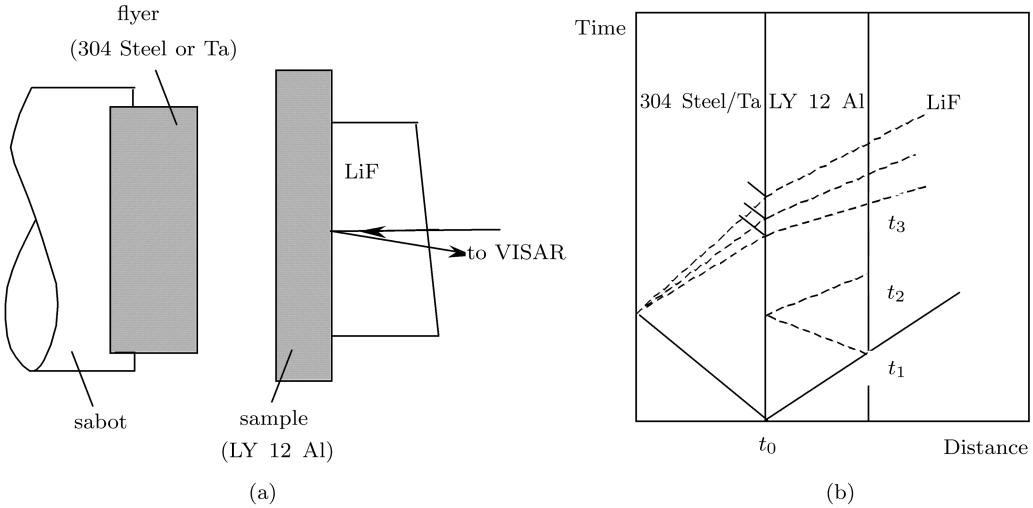


Fig.1. (a) Schematic of experimental setup for asymmetric plate impact and (b) time–distance diagram (in Lagrangian coordinates) of wave propagations after impact. (solid lines: shock waves; dashed lines: rarefaction waves).

Upon impact of the flyer on the LY12 Al sample at time t_0, a shock wave will propagate forward into the sample and another backward in the flyer plate. As seen in Fig.1(b), when the forward shock wave reaches the sample–window interface at time t_1, the interface particle speed history will jump up and a weak release wave will be reflected from the interface simultaneously because of the slight difference in impedance between the LY12 aluminium and the LiF window. This back-going weak rarefaction wave will be reflected again at the interface between the flyer plate and the sample and returns back to the sample–window interface at time t_2, a slight drop in the particle speed plateau will appear as the release wave reaches the interface. The longitudinal sound speed $c_{\rm l}$ of LY12 aluminium sample can then be obtained from the reverberation time interval between t_2 and t_1 in the particle speed history[12]

$$c_{\rm l} = \frac{\rho_0}{\rho}\left(\frac{2H_{\rm S}}{t_2 - t_1}\right), \qquad (2)$$

where ρ_0 is the initial density, ρ is the shock-compressed density, $H_{\rm s}$ is the initial thickness of the LY12 aluminium sample.

The backward shock wave in the flyer plate will be reflected as a rarefaction catch-up from the flyer–sabot interface. The catch-up rarefaction fan entering into the sample will interact with the sample–window interface at time t_3. The thicknesses of the flyer plate and the sample were so chosen that the catch-up rarefaction wave would arrive at the sample–window interface behind the arrival of the weak release produced by the forward-going shock waves, that is $t_3 > t_2$.

3. Results and discussion

Four asymmetric plate impact experiments were performed. The peak pressures in LY12 aluminium sample ranged from 85 to 131 GPa. A summary of the experimental conditions is presented in Table 1. Typical VISAR particle speed history is shown in Fig.2. As expected, the characteristic times t_1 and t_2 corresponding to those in Fig.1(b) are distinct and can easily be determined from the figure.

Table 1. Summary of asymmetric plate impact experiments.

Expt. No.	impact speed /(km/s)	flyer material	(flyer/sample/window) thicknesses /(mm)	peak pressure/(GPa)
1	5.15	Ta	2.032/1.120/11.0	110.0
2	5.81	Ta	1.968/1.151/11.0	131.0
3	4.76	HR2	3.007/1.580/11.0	84.6
4	5.58	HR2	3.008/1.587/11.0	106.0

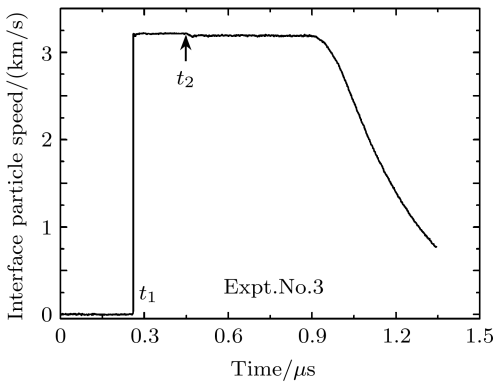


Fig.2. Typical interface particle speed history deduced from VISAR records (Expt. No.3). The times t_1 and t_2 correspond to the conditions labelled in Fig.1(b).

With the times t_1 and t_2 determined from Fig.2, the longitudinal sound speed $c_{\rm l}$ in LY12 aluminium was estimated from Eq.(2) with an uncertainty of ∼2%. The slight changes in shock pressure of the sample (about 2.3% at 131 GPa) caused by the reverberations of the rarefactions will in principle cause this sound speed to differ from the sound speed in the initial Hugoniot state. Considering the very small variations in pressure and density and an intrinsic uncertainty in experiment, however, this change can actually be neglected. The calculated longitudinal sound speeds as a function of shock pressure are shown in Fig.3. It can be seen that the longitudinal speed increases from 11.06 km/s at 84.6 GPa to 11.67 km/s at 110 GPa, then decreases to 11.34 km/s at 131 GPa. For aluminium, the shock-induced melting begins at 125 GPa and ends at about 150GPa.[17] The obvious decrease in sound speed implies that LY12 aluminium lies in a solid–liquid mixed phase regime at the highest pressure of 131 GPa.

Also shown in Fig.3 are the sound speed data given by Yu *et al*[16] for this material in a pressure range of 20–70 GPa, which were measured by VISAR

technique under symmetric impact conditions, and the data of McQueen *et al*[18] for 2024 aluminium in a pressure range of 55–145 GPa, which were measured by optical analyser technique. It can be seen that all of these data are shown to be consistent with each other. The longitudinal sound speeds along the Hugoniot in a solid phase region of both LY12 Al and 2024 Al can be described with extraordinary satisfaction by[19]

$$c_{\rm l} = 6.36 + 0.363P^{2/3} - 0.026P, \quad (3)$$

where $c_{\rm l}$ is in km/s and Hugoniot pressure P is in GPa. On the other hand, the longitudinal sound speed $c_{\rm l}$ in a solid–liquid mixed phase region (125–155 GPa) decreases gradually as the shock pressure increases.

The bulk sound speed $c_{\rm b}$ at the Hugoniot pressure P can be theoretically predicted via the Gruneisen EOS[20]

$$c_{\rm b} = \left\{ \frac{{\rm d}P}{{\rm d}\rho} \left[1 - \left(\frac{1}{\rho_0} - \frac{1}{\rho} \right) \frac{\rho\gamma}{2} \right] + \frac{P}{2} \left(\frac{\gamma}{\rho} \right) \right\}^{1/2}, \quad (4)$$

where ${\rm d}P/{\rm d}\rho$ is the local Hugoniot slope and γ is Gruneisen parameter. Product of $\rho\gamma$ is assumed to be constant for aluminium, which holds up to 400 GPa according to Nellies *et al*.[21] Our early results have shown that the bulk sound speed determined from the VISAR experiments is very consistent with those calculated from Gruneisen EOS by assuming $\rho\gamma$ = const.[16] We therefore calculate the bulk sound speed for the asymmetric impact experiments in the same way. The calculated bulk sound speeds are listed in Table 2.

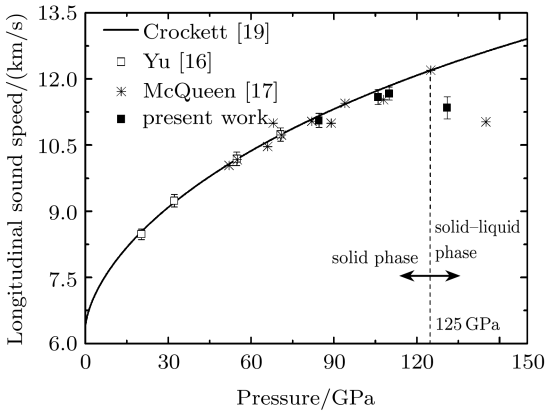


Fig.3. Longitudinal sound speeds as a function of shock pressure.

Table 2. Summary of experimental results and theoretical predictions.

P/GPa	Exp.			Steinberg model		Eq.(7)
	$c_{\rm l}$/(km/s)	$c_{\rm b}$ /(km/s)[c]	G/GPa[d]	η[e]	G/GPa[f]	G/GPa
20.3	8.48 [a]	6.80	63.8	1.19	58.8	60.8
32.1	9.24[a]	7.35	83.2	1.26	73.8	78.2
54.7	10.19[a]	8.14	108.8	1.38	97.4	107.6
70.6	10.73[a]	8.60	125.2	1.45	110.6	125.7
84.6	11.06[b]	8.95	133.6	1.50	120.2	139.7
106.0	11.59[b]	9.43	149.7	1.58	132.2	159.2
110.0	11.67[b]	9.52	151.6	1.59	134.1	162.6
131.0	11.34[b]	9.94	103.0	1.65	–	–

[a]Ref.[16].
[b]present work.
[c]calculated from Eq.(4) on the assumption that $\rho_0\gamma_0 = \rho\gamma$. $\rho_0 = 2.785\,{\rm g/cm^3}$ and $\gamma_0 = 2.0$.
[d]calculated from Eq.(1).
[e]calculated from Eq.(6) by using the relationship $D = 5.37{+}1.29u$.
[f]calculated from Eq.(5).

Using the longitudinal sound speed data determined experimentally and the bulk sound speed from Gruneisen EOS, the shear moduli of LY12 aluminium are calculated from Eq.(2), and they are summarized in Table 2. The variation of shear modulus with shock pressure is plotted in Fig.4. Also shown are the shear modulus data of 2024 aluminium obtained from the longitudinal sound speed data of McQueen *et al*[17] and the bulk sound speed from the Gruneisen EOS. It can be seen that the uniformity of the data between LY12 aluminium and 2024 aluminium is quite good. Figure 4 also demonstrates that while the shear modulus increases continuously with shock pressure until shock-induced melting occurs, it does not vanish immediately before complete melting happens. Instead, the gradual decrease of the shear modulus in a solid–

liquid mixed phase region under dynamic loading is totally different from the drastic dropping at the melting point under static conditions.

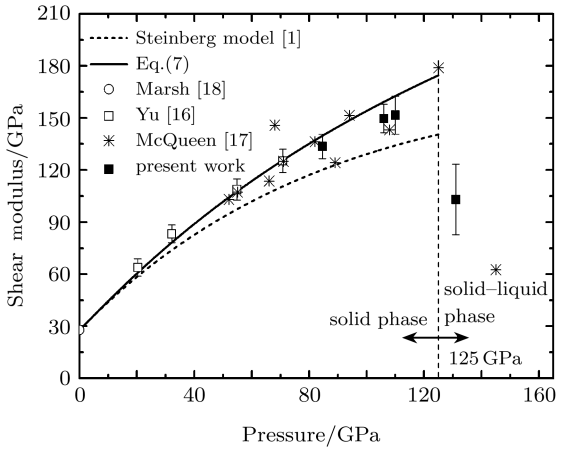


Fig.4. The variation of shear modulus with shock pressure, where a comparison between the Steinberg shear modulus model (Eq.(5)) and the modified model (Eq.(7)) is also indicated.

Various analytical models have been developed to describe shear modulus variations with pressure and temperature.[1,3,22–24] Of these models, the Steinberg shear modulus model is most often used in shock dynamics calculation. In his model, the shear modulus G is expressed as a function of pressure P and temperature T:

$$G(P,T) = G_0 \left[1 + \frac{G'_P}{G_0}\frac{P}{\eta^{1/3}} + \frac{G'_T}{G_0}(T - T_0)\right], \quad (5)$$

where η is the compression defined as the initial special volume V_0 divided by the special volume V under shock pressure P, G_0 is the shear modulus in a reference state ($T_0 = 300\,\mathrm{K}$, $P = 0$, $\varepsilon = 0$), G'_P and G'_T are derivatives of shear modulus with respect to pressure P and temperature T, respectively. For aluminium, Steinberg *et al*[1] gave these parameters as: $G_0 = 27.6\,\mathrm{GPa}$, $G'_P/G_0 = 65\,\mathrm{TPa}^{-1}$, $G'_T/G_0 = -0.62\,\mathrm{kK}^{-1}$。

Using the above parameters and the temperatures given by McQueen *et al*,[25] the pressure and the temperature dependences of the shear modulus for LY12 aluminium are calculated according to Eq.(5) up to 125 GPa.The results are also listed in Table 2 and plotted as a dashed curve against the shock pressure in Fig.4. A comparison of these data with the experimental data clearly shows that the Steinberg shear modulus model systematically underestimates the experimental results in a pressure range from about 20 to 125 GPa. The deviation of experimental results from the values given by the model becomes larger as shock pressure increases.

In the Steinberg shear modulus model,[1] the term $P/\eta^{1/3}$ is introduced to describe the pressure effect on shear modulus since, according to the Thomas–Fermi theory, $G \sim \eta^{4/3}$ and $P \sim \eta^{5/3}$ as $\eta \to \infty$. However, under shock loading conditions the compression η will not increase without limit even though the pressure goes infinitely. According to the Hugoniot relation derived from mass conservation, the compression η is related to particle speed u and shock speed D through[26]

$$\eta = \frac{V_0}{V} = \frac{D}{D-u} = \frac{1}{1-u/D}. \quad (6)$$

In the high-pressure limit, experimental results summarized by Trunin[27] show that the slope of Hugoniot, $s = \mathrm{d}D/\mathrm{d}u$, falls between 1.2 and 1.3 for most metals. This will yield a limit for shock compression $\eta = 4.3$–6.0. A compression of 3.9 ± 1.2 for aluminium at $3.2 \pm 0.5\,\mathrm{TPa}$ has also been reported in Ref.[27]. In fact, for shock compressions in a solid phase region, the pressure, and hence the compressibility, is still quite low and far from its limit condition. The values of compression η of LY12 aluminium estimated from Eq.(6) with the Hugoniot slope $s = 1.29$[18] are listed in Table 2. It can be seen from this table that the compression η falls between 1.19 and 1.64 over a shock pressure range of 20–131 GPa. A compression of 1.703 for 6061-T6 aluminium at 161GPa (in a liquid phase) has also been reported by Furnish *et al*.[28]

According to the above analyses, it is unreasonable to use $P\eta^{1/3}$ to describe the pressure effect on shear modulus G under shock loadings, since the value of compression η in a solid phase region is very limited and low. On the other hand, experiments show that shear modulus G varies linearly with pressure P in relatively low-pressure regions. We, therefore, propose to use a linear pressure term to describe the pressure dependence of shear modulus along the Hugoniot throughout the whole solid phase region. By replacing the non-linear pressure term of $P\eta^{1/3}$ in the Steinberg model, the modified equation is linear both in pressure and in temperature:

$$G = G_0 \left[1 + \left(\frac{G'_P}{G_0}\right) P + \left(\frac{G'_T}{G_0}\right)(T - 300)\right]. \quad (7)$$

Using the same parameters as those in Eq.(5) given by Steinberg *et al*,[1] the resulting equation is plotted in Fig.4 (solid curve). As illustrated in the figure, the

new shear modulus equation shows that it is consistent with the experimental data, implying that the shear modulus of the aluminium alloy varies linearly with pressure and temperature throughout the whole solid phase region.

4. Conclusions

Asymmetric plate impact experiments on LY12 aluminium by employing high-impedance flyer are conducted in a pressure range from 85 to 131 GPa. The sound speeds of LY12 aluminium are obtained from the time-resolved particle speed profiles deduced from the VISAR records, and they are shown to be in good agreement with our previous data and also with the results of 2024 aluminium reported by McQueen *et al*. The decrease of sound speed at 131 GPa is an indication that LY12 aluminium lies in a solid–liquid mixed phase region at this pressure.

By using the measured longitudinal sound speed data and the calculated bulk sound speed from Gruneisen EOS, the shear moduli of LY12 aluminium are determined in a pressure range from 20 to 131 GPa and show good coincidence with those of 2024 aluminium. The shear modulus of aluminium increases with shock pressure until shock-melting happens at 125GPa, and then decreases from 125 GPa onward. However, the gradually decrease of the shear modulus in a solid–liquid mixed phase region is very different from the drastic drop at the melting point under static conditions.

A comparison of the experimental results of shear modulus, including the data of 2024 aluminium, with the calculations based on the widely used shear modulus equation developed by Steinberg *et al* indicates that the estimations from the Steinberg shear modulus model are systematically lower than the experimental data from relatively low pressure of 20GPa to shock pressure of 125 GPa. We attribute this deviation to the inadequate term of $P/\eta^{1/3}$ in the Steinberg model. Using a linear pressure term to replace the term of $P/\eta^{1/3}$, we propose a modified shear modulus equation which has shown good consistence with the experimental data, implying that the shear modulus of LY12 aluminium varies linearly with pressure and temperature throughout the whole solid phase region.

References

[1] Steinberg D J, Cochran S G and Guinan M W 1980 *J. Appl. Phys.* **51** 1496

[2] Hu J B, Yu Y Y, Dai CH D and Tan H 2005 *Acta Phys. Sin.* **54** 5750 (in Chinese)

[3] Nadal M H and Poac P L 2003 *J. Appl. Phys.* **93** 2472

[4] Fraizier E and Nadal M H 2003 *J. Appl. Phys.* **93** 649

[5] McQueen R G, Hopson J W and Fritz J N 1982 *Rev. Sci. Instrum.* **53** 245

[6] Brown J M and Shaner J W In: Asay J R, Graham R A and Straub G K (ed) 1984 *Shock Waves in Condensed Matter-1983* (Amsterdam: North-Holland) p91

[7] Rosenberg Z 1986 *Rev. Sci. Instrum.* **57** 3107

[8] Rosenberg Z and Brar N S 1988 *Rev. Sci. Instrum.* **59** 991

[9] Barker L M and Hollenbach R E 1972 *J. Appl. Phys.* **43** 4669

[10] Martinez E and Servas J M In: Furnish M D, Thadhani N N and Horie Y (ed) 2002 *Shock Compression of Condensed Matter-2001* (New York: Melville) p1200

[11] Duffy T S and Ahrens T J 1997 *J. Appl. Phys.* **82** 4259

[12] Duffy T S and Ahrens T J 1995 *J. Geophys. Res.* **100** 529

[13] Asay J R and Chhabildas L C In: Meyers M M and Murr L E (ed) 1981 *Shock Waves and High-Strain-Rate Phenomena in Metals* (New York: Plenum) p417

[14] Bezruchkol G S, Kanel G I and Razorenov S V In: Furnish M D, Gupta Y M and Forbes J W (ed) 2004 *Shock Compression of Condensed Matter-2003* (New York: Melville) p29

[15] Hua J S, Jing F Q, Dong Y B and Tan H 2003 *Acta Phys. Sin.* **52** 2005 (in Chinese)

[16] Yu Y Y, Tan H, Hu J B, Dai CH D and Chen D N 2005 *Chin. Phys. Lett.* **22** 1742

[17] McQueen R G, Fritz J N and Morris C E In: Asay J R, Graham R A and Straub G K (ed) 1984 *Shock Waves in Condensed Matter* (Amsterdam: North-Holland) p95

[18] Marsh S P 1980 *LASL Shock Hugoniot Data* (Berkeley, CA: University of California Press) p166

[19] Crockett S, Chisolm E and Wallace D In: Furnish M D, Gupta Y M and Forbes J W 2004 *Shock Compression of Condensed Matter-2003* (New York: Melville) p45

[20] Ahrens T J In: Asay J R and Shahinpoor M (ed) 1992 *High-Pressure Shock Compression of Solids* (New York: Springer) p100

[21] Nellies W J, Mitchell A C and Yong D A 2003 *J. Appl. Phys.* **93** 304

[22] Straub G K 1991 LA-11806-MS

[23] Burakovsky L and Preston D L 2005 *Phys. Rev.* B **71** 184118

[24] Burakovsky L, Greeff C W and Preston D L 2003 *Phys. Rev.* B **67** 094107

[25] McQueen R G, Marsh S P, Taylor J W, Fritz J N and Carter W J In: Kinslow R (ed) 1970 *High-Velocity Impact Phenomena* (New York: Academic) p294

[26] Jing F Q 1999 *Introduction to Experimental Equation of State* (Beijing: Science Press) (in Chinese)

[27] Trunin R F 1998 *Shock Compression of Condensed Materials* (Cambridge: Cambridge University Press)

[28] Furnish M D, Chhabildas L C and Reinhart W D 1999 *Int. J. Impact Engng.* **23** 261